

## Conference Paper

# Synthesis, Crystal Structure, and Properties of $\text{NdNi}_{0.5}\text{Mn}_{0.5}\text{O}_{3-\delta}$ – A Possible Cathode Material for IT-SOFCs

A. Hossain, A. R. Gilev, E. A. Kiselev, and V. A. Cherepanov

Department of Physical and Inorganic Chemistry, Institute of Natural Sciences and Mathematics, Ural Federal University, 620002 Ekaterinburg, Russia

## Abstract

The crystal structure and properties of  $\text{NdNi}_{0.5}\text{Mn}_{0.5}\text{O}_{3-\delta}$  were studied in the temperature range of 25–1000°C in air. The perovskite-like monoclinic crystal structure ( $P2_1/n$ ) was stable at all studied temperatures.  $\text{NdNi}_{0.5}\text{Mn}_{0.5}\text{O}_{3-\delta}$  exhibited moderate thermal expansion with linear thermal expansion coefficient of  $10.12 \times 10^{-6} \text{ K}^{-1}$  (200–1000°C). Oxygen non-stoichiometry was almost temperature-independent in the whole temperature range studied with absolute value of 0.15 at room temperature. Total conductivity of the oxide was shown to be thermally activated with activation energy of 0.45 eV (350–1000°C) and the maximal value of 15 S/cm at 1000°C.

**Keywords:** manganite, crystal structure, oxygen non-stoichiometry, thermal expansion, total conductivity

Corresponding Author:

A. Hossain

aslam.hossain166@gmail.com

Received: 14 September 2018

Accepted: 1 October 2018

Published: 14 October 2018

Publishing services provided by  
Knowledge E

© A. Hossain et al. This article is distributed under the terms of the Creative Commons

Attribution License, which

permits unrestricted use and redistribution provided that the original author and source are credited.

Selection and Peer-review

under the responsibility of the ASRTU Conference Committee.

## 1. Introduction

The reduction of operating temperature of solid oxide fuel cells (SOFCs) down to the intermediate temperature range (600–800°C) is one of the main challenges for materials scientists today, which facilitates the development of new materials with improved performance. The  $\text{LaNiO}_3$ -related compounds have attracted considerable attention as an alternative to cobaltite due to their high electronic conductivity [1]. A relatively low thermodynamic stability of  $\text{LaNiO}_3$  can be improved by a partial substitution of Ni with such metals as Fe, Mn, or Ti [1, 2]. The studies of the  $\text{LaMn}_{1-y}\text{B}_y\text{O}_3$  perovskites (B = Co, Ni, Mg, Li) revealed that the catalytic activity can be enhanced by the substitution of Ni [3]. Moreover, the synergetic effect due to coexistence of two 3d-metals at the B-site in perovskite structure was observed when their concentrations were approximately equal [3]. This can be illustrated by a significant increase in catalytic activity in the  $\text{LaMn}_{1-x}\text{Cu}_x\text{O}_3$ ,  $\text{La}_{1-x}\text{Sr}_x\text{Mn}_{1-y}\text{Co}_y\text{O}_3$ , and  $\text{La}_{1-x}\text{Sr}_x\text{Co}_{1-y}\text{Fe}_y\text{O}_3$  systems [3].

## OPEN ACCESS

Recently,  $\text{La}_{1.80}\text{NiTiO}_{6-\delta}$  and  $\text{Pr}_2\text{NiMnO}_{6-\delta}$  were proposed as cathode materials for intermediate-temperature SOFCs (IT-SOFCs) [4, 5]. These compounds possessed perovskite-type monoclinic (sp.gr.  $P2_1/n$ ) crystal structure showing oxygen deficiency at room temperature. Both oxides exhibited relatively low values of total conductivity yielding  $\approx 0.002$  S/cm for  $\text{La}_{1.80}\text{NiTiO}_{6-\delta}$  and  $\approx 3$  S/cm for  $\text{Pr}_2\text{NiMnO}_{6-\delta}$  at  $800^\circ\text{C}$  in air. The activation energy of polarization resistance in the oxides was equal to 1.33 eV suggesting that the rate-limiting step of electrode processes was the charge transfer [5]. As a result,  $\text{Pr}_2\text{NiMnO}_{6-\delta}$  showed a better electrochemical performance with area-specific resistance (ASR) equal to  $0.38 \Omega \text{ cm}^2$  at  $700^\circ\text{C}$  against of  $\approx 0.5 \Omega \text{ cm}^2$  at  $800^\circ\text{C}$  for  $\text{La}_{1.80}\text{NiTiO}_{6-\delta}$ . The obtained ASR values were slightly better than those for the state-of-the-art LSM-based cathodes [5].

In this work,  $\text{NdNi}_{0.5}\text{Mn}_{0.5}\text{O}_{3-\delta}$  was studied as a potential cathode material for IT-SOFCs: crystal structure and functional properties were determined in the temperature range of  $25\text{--}1000^\circ\text{C}$  in air in order to assess the feasibility for practical application.

## 2. Methods

$\text{NdNi}_{0.5}\text{Mn}_{0.5}\text{O}_{3-\delta}$  was synthesized by a citrate-nitrate combustion technique described elsewhere [6]. The obtained powder was calcined at  $1100^\circ\text{C}$  for 20 h, uniaxially pressed into pellets under a pressure of 20 bar and sintered at  $1200^\circ\text{C}$  for 15 h in air. The phase composition and crystal structure were analyzed by X-ray powder diffraction (XRPD) using XRD-7000 Maxima instrument (Shimadzu) with  $\text{Cu-K}_\alpha$  radiation at RT. High-temperature XRPD (HT-XRPD) was performed in air within the  $30\text{--}1000^\circ\text{C}$  temperature range using HTK 1200N (Anton Paar) HT-chamber. The XRPD patterns were refined by the Rietveld method using FullProf software.

The temperature dependence of oxygen non-stoichiometry for  $\text{NdNi}_{0.5}\text{Mn}_{0.5}\text{O}_{3-\delta}$  was obtained by thermogravimetric analysis (TGA) using a Netzsch STA 409 PC instrument in the temperature interval of  $25\text{--}1100^\circ\text{C}$ . The absolute value of oxygen content at room temperature was calculated from the results of iodometric titration performed with Akvilon (ATP-o2) as described previously [7]. The total conductivity and Seebeck coefficient measurements were carried out simultaneously using the standard 4-probe DC technique with Pt wire leads. The data were collected in the temperature range of  $25\text{--}1000^\circ\text{C}$  on cooling with steps of  $50^\circ\text{C}$  in air.

### 3. Results

The XRPD pattern of as-sintered  $\text{NdNi}_{0.5}\text{Mn}_{0.5}\text{O}_{3-\delta}$  refined by the Rietveld method is shown in Figure 1. The initial structural model was based on the data reported in [6] and included the main monoclinic phase (sp.gr.  $P2_1/n$ ) and an impurity of NiO (sp.gr.  $Fm3m$ ). Figure 1 demonstrates that calculated curve satisfactorily describes the experimental data with  $R_B$  and  $R_f$  factors  $< 5\%$ . The amount of NiO in the sample was shown to be  $\approx 1\%$ . The structural and lattice parameters, together with the selected bond lengths are presented in Table 1. The refined crystal structure parameters are in good agreement with those reported earlier [4, 5, 8]. Previously,  $\text{NdNi}_{0.5}\text{Mn}_{0.5}\text{O}_3$  was studied by neutron powder diffraction (NPD) at 210 K in air [8]. It crystallized in a monoclinic  $P2_1/n$  structure containing two different octahedral positions (occupied by Ni and Mn) and was shown to be oxygen stoichiometric. Sánchez-Benítez et al. explained it by the charge disproportionation process  $\text{Ni}^{3+} + \text{Mn}^{3+} \rightarrow \text{Ni}^{2+} + \text{Mn}^{4+}$  and stated that from the structural point of view this compound could be considered as a double perovskite of composition  $\text{Nd}_2\text{NiMnO}_6$  [8]. However, the degree of long-range ordering between Ni and Mn sites was equal to 88.4%. In this work, the obtained bond lengths (Table 1) also suggested that the majority of cation species existed in a form of  $\text{Ni}^{2+}$  and  $\text{Mn}^{4+}$ , although small amounts of  $\text{Ni}^{3+}$  and  $\text{Mn}^{3+}$  could be present. Taking into account these observations, one should conclude that subtle monoclinic distortions in  $\text{NdNi}_{0.5}\text{Mn}_{0.5}\text{O}_3$  occur due to different size of  $\text{MO}_6$  octahedra surrounding Ni and Mn, which are statistically located one after another (as a result of their equal concentrations) in three directions of the perovskite network.

The HT-XRPD profiles of  $\text{NdNi}_{0.5}\text{Mn}_{0.5}\text{O}_{3-\delta}$  (Fig. 2) indicated that the monoclinic phase was stable up to 1000°C in air with no structural transitions observed in the temperature range studied. The overlapping of peaks with temperature near 32.8° (inset in Figure 2) can be explained by an increase in unit cell parameters resulting in the shifting of peaks toward the smaller  $2\theta$  values. The refined lattice parameters as a function of temperature are presented in Figure 3. As can be seen from Figure 3, the unit cell expands predominantly in  $a$  and  $c$  directions. The Me–O bond lengths analysis revealed that strong distortion of the  $\text{MnO}_6$  octahedra might be responsible for the observed anisotropy. The thermal expansion coefficients (TECs) for unit cell parameters were determined from the slopes of the corresponding temperature dependencies as previously described in [6]. The LTEC was estimated in approximation of non-textured polycrystalline material with randomly oriented crystallites [6, 9]. The calculated TEC values are summarized in Table 2, together with TECs of  $\text{Pr}_2\text{NiMnO}_{6-\delta}$

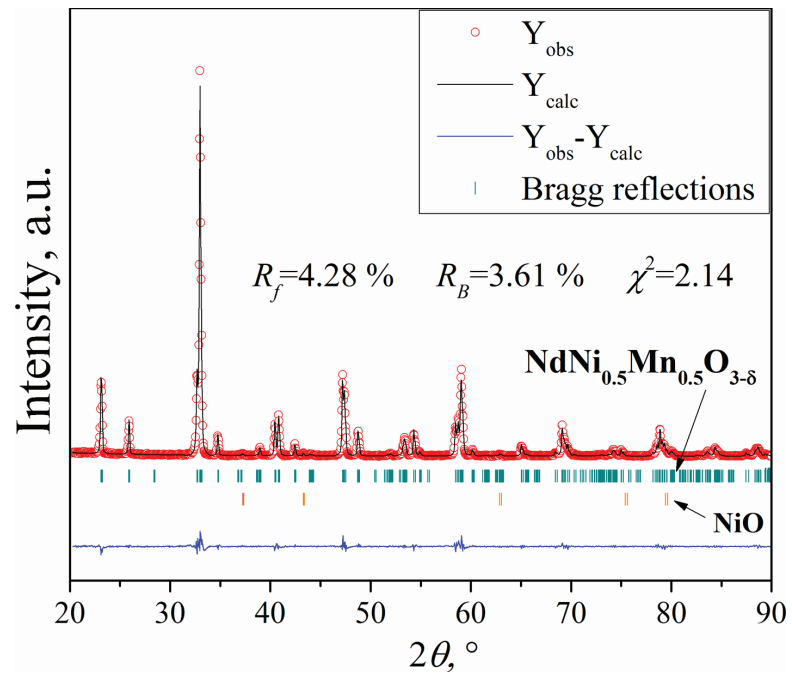


**Figure 1:** XPRD pattern of  $\text{NdNi}_{0.5}\text{Mn}_{0.5}\text{O}_{3-\delta}$  at room temperature refined by the Rietveld method.

**TABLE 1:** The unit cell parameters, structural parameters and selected Me–O bond lengths for the monoclinic  $\text{NdNi}_{0.5}\text{Mn}_{0.5}\text{O}_{3-\delta}$  phase at room temperature obtained by the Rietveld method. sp. gr.  $P2_1/n$ ,  $a = 5.4078(1)$  Å,  $b = 5.4792(1)$  Å,  $c = 7.6662(1)$  Å,  $V = 227.152(7)$  Å<sup>3</sup>,  $\beta = 90.069^\circ$ .

Atom	Site	Refined coordinates			Selected bonds	Bond length, Å
		<i>x</i>	<i>y</i>	<i>z</i>		
<b>Nd</b>	4e	−0.0091(6)	0.0441(2)	0.250(1)	Nd–O1 Nd–O2 Nd–O3	2.38(2) 2.40(5) 2.39(4)
<b>Ni</b>	2c	0.5	0	0.5	Ni–O1 Ni–O2 Ni–O3	2.09(5) 2.14(4) 2.11(4)
<b>Mn</b>	2d	0.5	0	0	Mn–O1 Mn–O2 Mn–O3	1.83(5) 1.81(4) 1.83(4)
<b>O1</b>	4e	0.074(4)	0.482(3)	0.268(5)		
<b>O2</b>	4e	0.690(8)	0.265(8)	0.044(6)		
<b>O3</b>	4e	0.727(8)	0.309(6)	0.461(6)		

[4] and  $\text{La}_{0.95}\text{Ni}_{0.5}\text{Ti}_{0.5}\text{O}_{3-\delta}$  [10]. The LTEC value for  $\text{NdNi}_{0.5}\text{Mn}_{0.5}\text{O}_{3-\delta}$  correlates well with LTECs of  $\text{Pr}_2\text{NiMnO}_{6-\delta}$  and  $\text{La}_{0.95}\text{Ni}_{0.5}\text{Ti}_{0.5}\text{O}_{3-\delta}$  showing moderate thermal expansion compatible with that for well-known electrolyte materials [1].

The oxygen non-stoichiometry in  $\text{NdNi}_{0.5}\text{Mn}_{0.5}\text{O}_{3-\delta}$  was essentially temperature-independent in whole temperature range studied with average value of  $0.15 \pm 0.02$  at

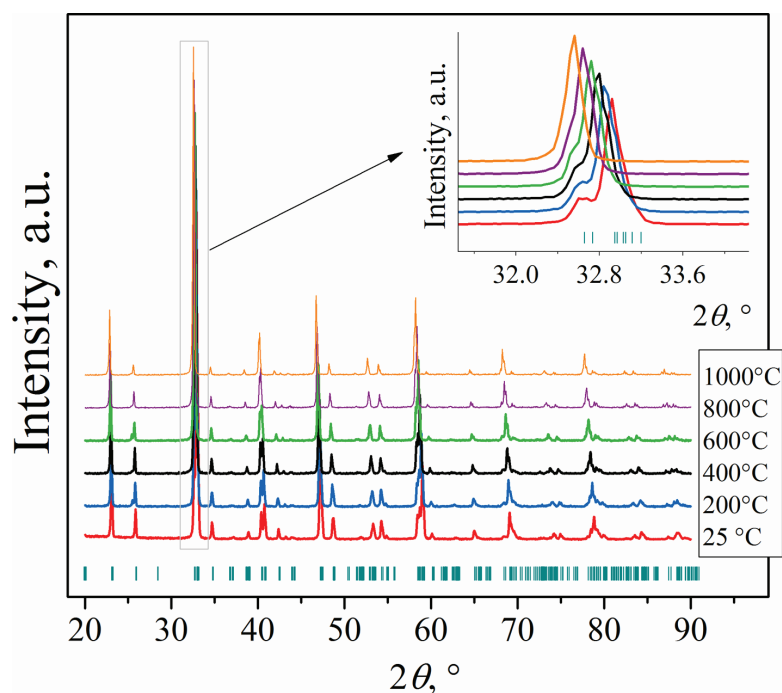
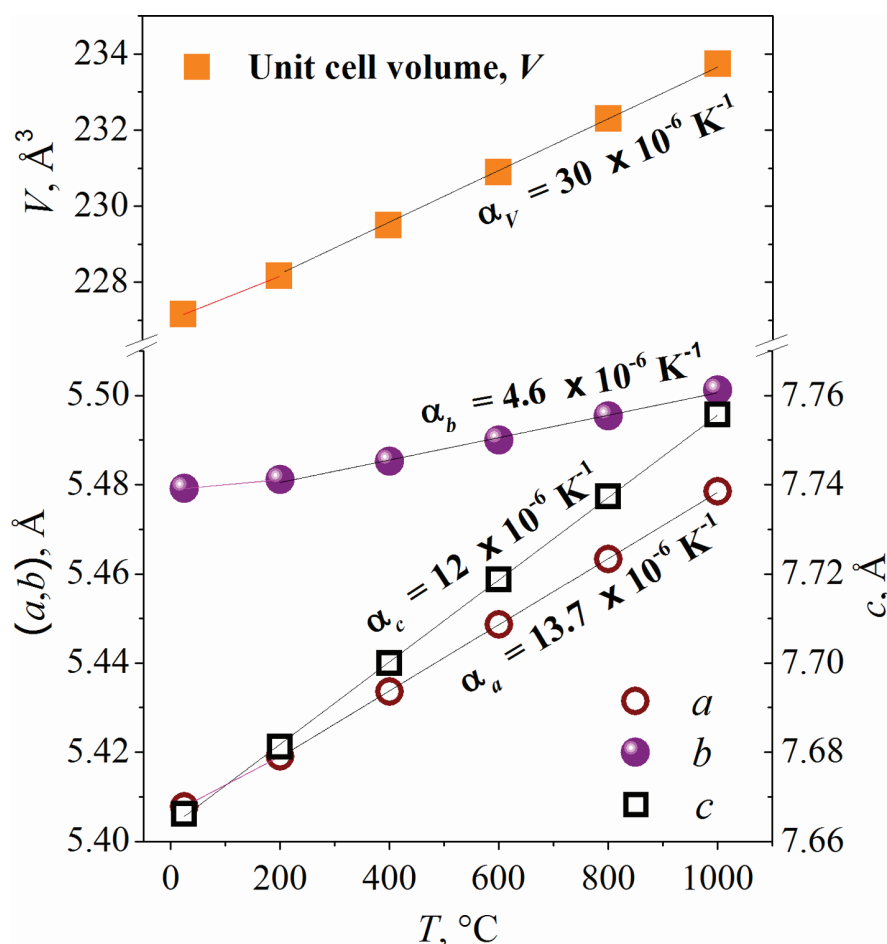


Figure 2: HT-XPRD patterns of  $\text{NdNi}_{0.5}\text{Mn}_{0.5}\text{O}_{3-\delta}$ .

TABLE 2: TEC values for  $\text{NdNi}_{0.5}\text{Mn}_{0.5}\text{O}_{3-\delta}$  and related materials in air.

$\text{NdNi}_{0.5}\text{Mn}_{0.5}\text{O}_{3-\delta}$	T = 25–200°C	T = 200–1000°C
$\alpha_V \times 10^6, \text{K}^{-1}$	25.2	$29.98 \pm 0.5$
$\alpha_a \times 10^6, \text{K}^{-1}$	11.87	$13.73 \pm 0.05$
$\alpha_b \times 10^6, \text{K}^{-1}$	2.05	$4.58 \pm 0.17$
$\alpha_c \times 10^6, \text{K}^{-1}$	$12.04 \pm 0.07$	$12.04 \pm 0.07$
$\alpha_L \times 10^6, \text{K}^{-1}$	8.65	$10.12 \pm 0.19$
$\text{Pr}_2\text{NiMnO}_{6-\delta}$ [5]	T = 50–800°C	
$\alpha_L \times 10^6, \text{K}^{-1}$	10.6	
$\text{La}_{0.95}\text{Ni}_{0.5}\text{Ti}_{0.5}\text{O}_{3-\delta}$ [10]	T = 250–650°C	T = 750–950°C
$\alpha_L \times 10^6, \text{K}^{-1}$	$9.99 \pm 0.01$	$11.96 \pm 0.01$

room temperature. Similar temperature dependence was also found in  $\text{La}_{0.95}\text{Ni}_{0.5}\text{Ti}_{0.5}\text{O}_{3-\delta}$  [10], although the oxygen deficit observed in  $\text{NdNi}_{0.5}\text{Mn}_{0.5}\text{O}_{3-\delta}$  was higher compared to that reported in [8], where  $\text{NdNi}_{0.5}\text{Mn}_{0.5}\text{O}_{3-\delta}$  was shown to be oxygen stoichiometric within standard deviations at 210 K in air by means of NPD. The increased oxygen deficiency in the obtained sample could be a result of cation non-stoichiometry at the A- and/or B-site, which was earlier observed for  $\text{La}_{2-x}\text{NiTiO}_{6-\delta}$  [4, 10]. Indeed, such A-site deficiency can be assumed, since trace amounts of NiO were observed in the studied sample.



**Figure 3:** Temperature dependencies of the unit cell parameters ( $a$ ,  $b$ ,  $c$ ) and the unit cell volume ( $V$ ) in  $\text{NdNi}_{0.5}\text{Mn}_{0.5}\text{O}_{3-\delta}$ .

The total conductivity ( $\sigma$ ) of  $\text{NdNi}_{0.5}\text{Mn}_{0.5}\text{O}_{3-\delta}$  showed semiconducting-like behavior in the whole temperature range studied (Fig. 4). The  $\sigma$  value of 7.3 S/cm was obtained at 800°C, which was slightly higher than 5.7 S/cm reported for  $\text{Pr}_2\text{NiMnO}_{6-\delta}$  at this temperature [5]. The maximal value of 15 S/cm was reached at 1000°C. The  $\ln(\sigma T) = f(1/T)$  plot (inset in Figure 4) revealed that charge transfer was thermally activated suggesting a small polaron hopping mechanism. The activation energy increased with temperature from 0.34 eV ( $T < 350^\circ\text{C}$ ) to 0.45 eV ( $T > 350^\circ\text{C}$ ). Similar behavior was also observed for  $\text{Pr}_2\text{NiMnO}_{6-\delta}$  at 550°C [5]. It could be explained by the gradual elongation of Ni–O–Mn bond lengths with temperature (for instance, the Ni–O1–Mn bond length increased from 3.83 Å at room temperature to 3.85 Å and 3.88 Å at 400 and 1000°C, respectively). The Seebeck coefficient ( $S$ ) of  $\text{NdNi}_{0.5}\text{Mn}_{0.5}\text{O}_{3-\delta}$  (inset in Figure 4) possessed complex temperature dependence and adopted negative values at all studied temperatures showing that predominant charge carriers in the oxide were electrons localized on  $\text{Ni}^{3+}$  cations forming  $\text{Ni}^{2+}$ .

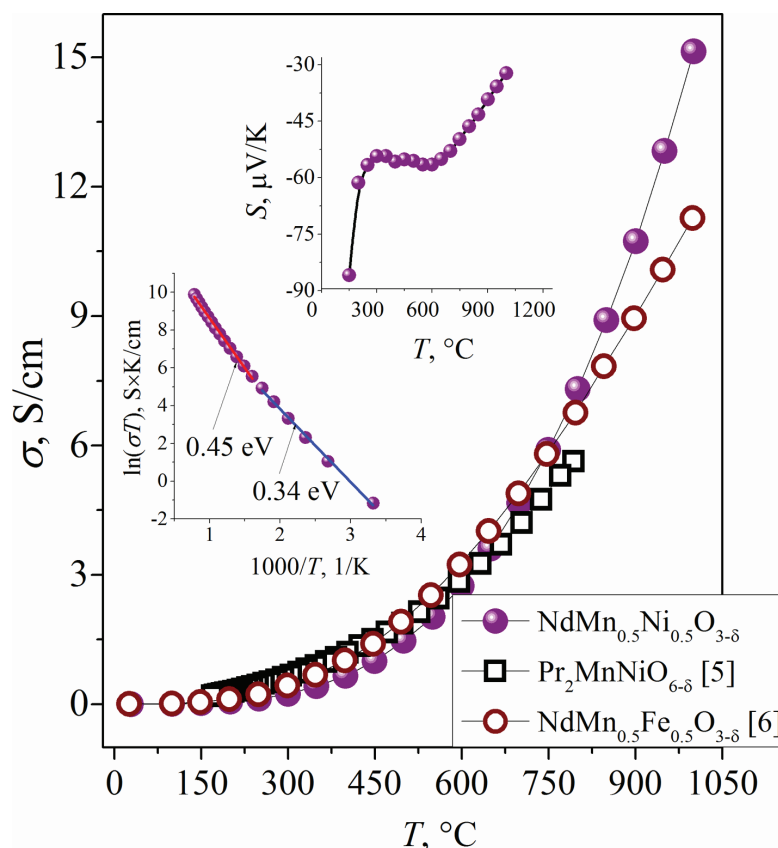


**Figure 4:** Temperature dependencies of total conductivity ( $\sigma$ ) and Seebeck coefficient ( $S$ ) for  $\text{NdNi}_{0.5}\text{Mn}_{0.5}\text{O}_{3-\delta}$  in air.

## 4. Conclusion

$\text{NdNi}_{0.5}\text{Mn}_{0.5}\text{O}_{3-\delta}$  possessed monoclinic crystal structure (sp. gr.  $P2_1/n$ ) in the temperature range of 25–1000°C. This complex oxide showed moderate thermal expansion with LTEC value equal to  $10.12 \times 10^{-6} \text{ K}^{-1}$  (200–1000°C), which is compatible with such well-known electrolytes as  $(\text{Y}_2\text{O}_3)_{0.08}(\text{ZrO}_2)_{0.92}$ ,  $\text{Ce}_{0.8}\text{Sm}_{0.2}\text{O}_{1.9}$ , and  $\text{La}_{0.9}\text{Sr}_{0.1}\text{Ga}_{0.8}\text{Mg}_{0.2}\text{O}_{2.85}$  [1]. Moreover, the chemical expansion contribution is negligible due to temperature-independent oxygen non-stoichiometry. On the one hand, the latter fact is a notable advantage of this material compared with known cobalt-based cathodes. On the other hand, one could expect low oxygen-ion transport [10, 11] in  $\text{NdNi}_{0.5}\text{Mn}_{0.5}\text{O}_{3-\delta}$  due to temperature-independent oxygen content.

$\text{NdNi}_{0.5}\text{Mn}_{0.5}\text{O}_{3-\delta}$  showed semiconductor-like behavior in the whole temperature range studied with maximum value of conductivity  $\approx 15 \text{ S/cm}$  at 1000°C. The total conductivity in  $\text{NdNi}_{0.5}\text{Mn}_{0.5}\text{O}_{3-\delta}$  was slightly higher than that for  $\text{Pr}_2\text{NiMnO}_{6-\delta}$ , although it was still significantly lower compared with a preferable value ( $> 100 \text{ S/cm}$ ) for the IT-SOFCs cathodes [1]. Bulk oxygen diffusion, surface oxygen exchange, and chemical

compatibility of  $\text{NdNi}_{0.5}\text{Mn}_{0.5}\text{O}_{3-\delta}$  with well-known electrolytes should be studied in the future in order to make a conclusion on possibility of its application as a cathode material for IT-SOFCs.

## Acknowledgement

The authors would like to acknowledge that the equipment of the Ural Center for Shared Use 'Modern nanotechnology' SNSM UrFU was used in this research.

## Funding

This work was supported in parts by the Ministry of Education and Science of the Russian Federation (State Task 4.2288.2017) and by Act 211 Government of the Russian Federation, agreement 02.A03.21.0006.

## References

- [1] Sun, C., Hui, R., and Roller, J. (2010). Cathode materials for solid oxide fuel cells: A review. *Journal of Solid State Electrochemistry*, vol. 14, pp. 1125–1144.
- [2] Chiba, R., Yoshimura, F., and Sakurai, Y. (1999). An investigation of  $\text{LaNi}_{1-x}\text{Fe}_x\text{O}_3$  as a cathode material for solid oxide fuel cells. *Solid State Ionics*, vol. 124, pp. 281–288.
- [3] Yamazoe, N. and Teraoka, Y. (1990). Oxidation catalysis of perovskites – Relationships to bulk structure and composition (valency, defect, etc.). *Catalysis Today*, vol. 8, pp. 175–199.
- [4] Pérez-Flores, J. C., Pérez-Coll, D., García-Martín, S., et al. (2013). A- and B-site ordering in the A-cation-deficient perovskite series  $\text{La}_{2-x}\text{NiTiO}_{6-\delta}$  ( $0 \leq x < 0.20$ ) and evaluation as potential cathodes for solid oxide fuel cells. *Chemistry of Materials*, vol. 25, pp. 2484–2494.
- [5] Li, H., Sun, L. P., Li, Q., et al. (2015). Electrochemical performance of double perovskite  $\text{Pr}_2\text{NiMnO}_6$  as a potential IT-SOFC cathode. *International Journal of Hydrogen Energy*, vol. 40, pp. 12761–12769.
- [6] Gilev, A. R., Hossain, A., Kiselev, E. A., et al. (2018). A-site substitution effect on crystal structure and properties of  $\text{Nd}_{1-x}\text{A}_x\text{Mn}_{0.5}\text{Fe}_{0.5}\text{O}_{3-\delta}$  ( $\text{A}=\text{Ca}, \text{Sr}, \text{Ba}$ ;  $x=0, 0.25$ ). *Solid State Ionics*, vol. 323, pp. 67–71.



- [7] Kundu, A. K., Mychinko, M. Y., Caignaert, V., et al. (2015). Coherent inter-growth of simple cubic and quintuple tetragonal perovskites in the system  $\text{Nd}_{2-\epsilon}\text{Ba}_{3+\epsilon}(\text{Fe,Co})_5\text{O}_{15-\delta}$ . *Journal of Solid State Chemistry*, vol. 231, pp. 36–41.
- [8] Sánchez-Benítez, J., Martínez-Lope, M. J., Alonso, J. A., et al. (2011). Magnetic and structural features of the  $\text{NdNi}_{1-x}\text{Mn}_x\text{O}_3$  perovskite series investigated by neutron diffraction. *Journal of Physics: Condensed Matter*, vol. 23, p. 226001.
- [9] Munnings, C. N., Skinner, S. J., Amow, G., et al. (2006). Structure, stability and electrical properties of the  $\text{La}_{(2-x)}\text{Sr}_x\text{MnO}_{4\pm\delta}$  solid solution series. *Solid State Ionics*, vol. 177, pp. 1849–1853.
- [10] Yakovlev, S., Kharton, V., Yaremchenko, A., et al. (2007). Mixed conductivity, thermal expansion and defect chemistry of A-site deficient  $\text{LaNi}_{0.5}\text{Ti}_{0.5}\text{O}_{3-\delta}$ . *Journal of the European Ceramic Society*, vol. 27, pp. 4279–4282.
- [11] Kato, S., Kikawa, D., Ogasawara, M., et al. (2005). Synthesis and oxygen permeability of the perovskite-type oxides in the La-Sr-Fe-Mn-O system. *Solid State Ionics*, vol. 176, pp. 1377–1381.